Available online at www.sciencedirect.com
ScienceDirect
Thermochimica Acta 454 (2007) 99–108
thermochimica acta
www.elsevier.com/locate/tca

Thermodynamic study of the *n*-octane-1-pentanol-sodium dodecyl sulfate solutions in water

Nikolai G. Polikhronidi [a], Genadii V. Stepanov [a], Ilmutdin M. Abdulagatov [b,*], Rabiyat G. Batyrova [a]

[a] *Institute of Physics of the Dagestan Scientific Center of the Russian Academy of Sciences, 367005 Makhachkala, M. Yaragskogo Str. 94, Dagestan, Russia*
[b] *Institute for Geothermal Problems of the Dagestan Scientific Center of the Russian Academy of Sciences, 367003 Makhachkala, Shamilya Str. 39-A, Dagestan, Russia*

Received 1 August 2006; received in revised form 12 December 2006; accepted 17 December 2006
Available online 22 December 2006

Abstract

The thermodynamic properties, $PVTx$ (T_S, P_S, ρ_S), $(\partial P/\partial T)_{VX}$, and $C_V VTx$, of three microemulsions (water + *n*-octane + sodium dodecylsulfate + 1-pentanol) with composition of solution-1: 0.0777 (H_2O):0.6997 (*n*-C_8H_{18}):0.0777 (SDS):0.1449 (1-$C_5H_{11}OH$) mass fraction; solution-2: 0.6220 (H_2O):0.1555 (*n*-C_8H_{18}):0.0777 (SDS):0.1448 (1-$C_5H_{11}OH$) mass fraction; and solution-3: 0.2720 (H_2O):0.5054 (*n*-C_8H_{18}):0.0777 (SDS):0.1449 (1-$C_5H_{11}OH$) mass fraction were measured. Sodium dodecylsulfate (SDS) was used as an ionic surfactant, 1-pentanol used as stabilizer (cosurfactant), and *n*-octane as oil component in aqueous solution. A high-temperature, high-pressure, adiabatic, and nearly constant-volume calorimeter supplemented by quasi-static thermogram technique was used for the measurements. Measurements were made at eight densities (isochores) between 475.87 and 919.03 kg m^{-3}. The range of temperature was from 275 to 536 K and pressure range was up to 138 bar. Uncertainty of the pressure, density, derivative $(\partial P/\partial T)_{VX}$, and heat capacity measurements are estimated to be 0.25%, 0.02%, 0.12–1.5%, and 2.5%, respectively. Temperatures at liquid–gas phase transition curve, $T_S(\rho)$, for each measured densities (isochores) were determined using a quasi-static thermogram technique. The uncertainty of the phase transition temperature measurements is about ±0.02 K. The effect of temperature, density, and concentration on the heat capacity of the microemulsions is discussed. Along the isochore of 438.40 kg m^{-3} at temperatures above 525.44 K for the first solution the precipitation of the solid phase (SDS) was found.

Keywords: Adiabatic calorimeter; Density; Heat capacity; *n*-Octane; 1-Pentanol; Phase transition; Pressure; Sodium dodecylsulfate; Water

1. Introduction

Aqueous solutions containing the surfactant are important for many practical applications. For example, the surfactants are used for the enhanced oil recovery and detergency and improving the understanding of surfactants effect on this process have practical importance. The modeling and prediction of the process of tertiary oil recovery or the condition of the solubilization of hydrocarbons in ternary systems generally formed with water, a surfactant (SDS), and a cosurfactant (alcohol) are required knowledge accurate thermodynamic properties and phase diagram data for quaternary system, microemulsion (water + surfactant (SDS) + alcohol + hydrocarbon). Microemulsion systems are very important in biology, medicine, and environment, and in tertiary oil recovery processes [1–5]. Less attention has been paid to the thermodynamic of the solutions with surfactant on the especially direct measurements of the different properties as functions of concentration, temperature, and pressure. Volumetric and calorimetric data are great important since they can be used test theories and models and to obtain information on the interaction governing the micelles formation in different liquid media.

Isochoric heat capacity is one of the important thermodynamic characteristics of fluids and fluid mixtures in phase transition phenomena study. Constant-volume calorimeter provides a useful method for the study of phase transition

* Corresponding author. Present address: Physical and Chemical Properties Division, National Institute of Standards and Technology, 325 Broadway, Boulder, CO 80305, USA. Tel.: +1 303 497 4027; fax: +1 303 497 5224.
E-mail address: ilmutdin@boulder.nist.gov (I.M. Abdulagatov).

0040-6031/$ – see front matter © 2006 Elsevier B.V. All rights reserved.
doi:10.1016/j.tca.2006.12.014

phenomena in complicated multicomponent solutions. In this work, we use the fact that a constant-volume heat capacity C_V is a very sensitive indicator of phase changes [6–17]. Therefore, the constant-volume heat capacity C_V can be a very sensitive tool that determines various type liquid–solid (L–S), liquid–liquid (L–L), liquid–vapor (L–V), solid–vapor (S–V), liquid–solid–vapor (L–S–V), liquid–liquid–solid (L–L–S), and liquid–liquid–vapor (L–L–V) phase transitions occurring in a complex fluid mixtures heated in a closed volume. The discontinuity in C_{VX} behavior at the intersection of the phase boundary curve are connected with various type phase transitions (L–L, L–V, L–S, V–S, L–L–S, L–L–V, and L–S–V) occurring in a complicated fluid mixtures heated in a closed volume. Isochoric heat capacity C_V measurements improve our understanding of many important phenomena taking place in complex multicomponent mixtures near the phase transition points. Isochoric heat capacity experiments enable one to accurately determine the phase transition temperatures T_S of the system from the one- to the two-phase, from the two- to the three-phase state and vice versa [18,19]. The technique of determining phase boundary parameters (T_S, P_S, ρ_S, x) (L–V, L–L–V, and L–V–S) is described in our previous publications [6–17]. Fig. 1 shows schematic representation of the general behavior of isochoric heat capacity C_V as a function of specific volume V at fixed sub-critical isotherm ($T < T_C$) in the vapor (one-phase), liquid (one-phase), and vapor–liquid (two-phase) phases. The heat capacity C_V jumpily decreases or increases on passing through the phase transition points while heating isochorically. Thus, the phase transition observed can mark only the disappearance one of the phase (vapor, liquid, solid) (L–V ⇔ L, L–V ⇔ V, L–G–V ⇔ L–V, L–V–S ⇔ L–S, L–V–S ⇔ V–S). At the phase transition, the density of the liquid solution is readily calculated from the volume of the calorimeter and the mass of the solution (see below). This technique will be used in this work to study the two-phase (L–V) boundaries for the complex quaternary mixtures of water + *n*-octane + SDS + 1-pentanol. Some authors have used a break-point technique (*P–V* and *P–T* break points) in a *PVTx* experiment to study phase boundary curves in aqueous salt solutions (see for example [20–22]). While this method can be quite reliable, its precision can be improved upon by applying a sensitive calorimetric technique.

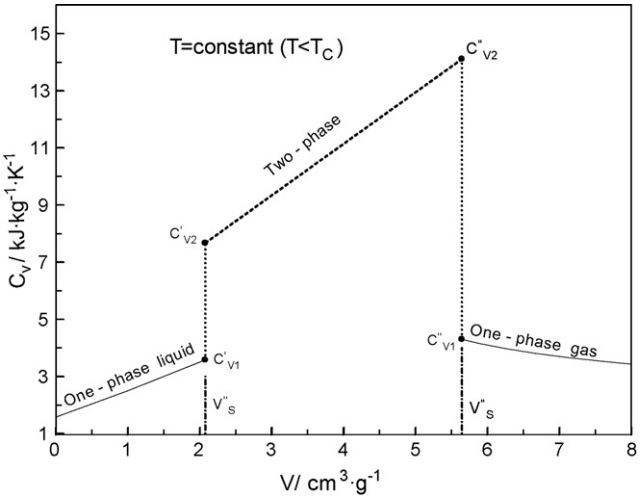

Fig. 1. Typical isochoric heat capacity behavior as a function of specific volume ($V = 1/\rho$) along constant temperature ($T < T_C$). C'_{V1}: one-phase liquid isochoric heat capacity at the phase transition point, C'_{V2}: two-phase liquid isochoric heat capacity at the phase transition point, C''_{V1}: one-phase vapor isochoric heat capacity at the phase transition point, C''_{V2}: two-phase vapor isochoric heat capacity at the phase transition point, V'_S: specific volume of liquid at the liquid–gas phase transition point (saturated liquid volume), V'_S: specific volume of the gas at the liquid–gas phase transition point (saturated gas volume).

The primary objective of this work is to provide accurate experimental volumetric (*PVTx*), $(\partial P/\partial T)_{VX}$, calorimetric ($C_V VTx$), and phase boundary ($T_S$, P_S, ρ_S, x) properties data for complex quaternary fluid mixtures (microemulsion). The microemulsion has been formed by mixing water, surfactant (SDS), cosurfactant (1-pentanol), and hydrocarbon (*n*-octane), water + n-octane + SDS + 1-pentanol. In this system SDS is surfactant used as component in stabilizing the microemulsion, alcohol (1-pentanol) used as cosurfactant. As typical oil, *n*-octane was used. Surfactant favors the formation and the stabilization of alcohol microaggregates. The cosurfactant used is very essential to increase the solubilization of hydrocarbons in water. Calorimetric studies are efficient method for investigating of the microemultions and provide very useful information about microstructure of the system, to understand the mechanism of formation of different structural zones in the microemulsion phase diagram. These zones play very essential role in determination optimal conditions for the maximum solubilizing oil in water. The concentration of the surfactant and cosurfactant play also very essential role in solubilizing of oil in water. It is the purpose of this paper to accurate determine the locations of the phase boundaries (phase behavior) encountered from 275 to 536 K, as they manifest themselves in peaks and jumps in the heat capacity or isochoric *P–T* break point data for water + *n*-octane + SDS + 1-pentanol. In our previous papers [18,19] we used this technique to accurately determine the location of the L–V, L–L–V and L–S–V phase transition curves for complicated multicomponent thermodynamic systems such as water + hydrocarbon and water + salt. Fig. 2 shows the typical C_V–T curves for two complicated mixtures (partially miscible mixture H_2O + *n*-C_6H_{14} [19] and H_2O + Na_2SO_4 [18] solution with salt precipitation at high temperatures, type 2 aqueous solution) near the two different types of phase transition points. In Fig. 2 first and second peaks indicates the occurrence of two different type phase transitions (L–L, L–V and L–S, L–V). First peak is observed when second liquid disappears (Fig. 2a) and when salt first precipitates (Fig. 2b) and, on further heating, a second lambda-shaped peak is seen when the vapor or liquid phase disappears.

Previously some thermodynamic properties (density, heat capacity at constant pressure) for microemulsions (water + alcohol + hydrocarbon + surfactant) were studied by several authors [23–26]. The density (ρ) and heat capacity at constant pressure (C_P) of microemulsion formed by water + SDS + *n*-butanol + toluene has been studied by Roux et al. [23] and Roux-Desgranges et al. [24] at room temperature (25 °C). These properties for the ternary system (water + SDS + *n*-butanol) and (water + toluene + *n*-butanol) were studied by the same authors Roux-Desgranges et al. [25]

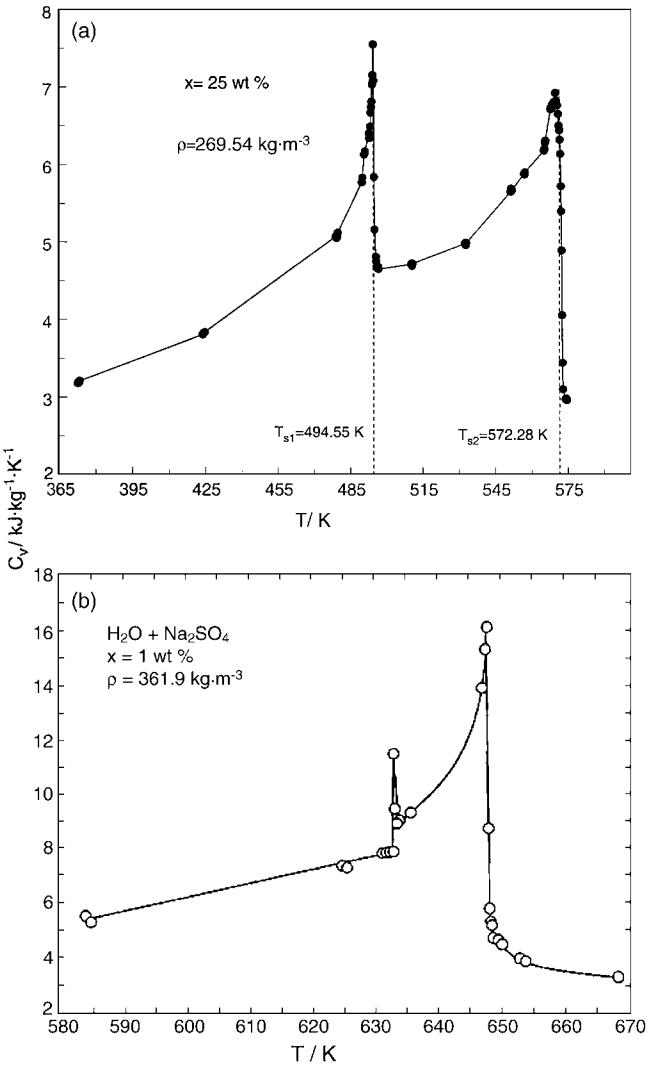

Fig. 2. Isochoric heat capacity of $H_2O + n\text{-}C_6H_{14}$ mixture (a) and $H_2O + Na_2SO_4$ solution (b) as a function of temperature along the constant density and concentration near the phase transition points. (a) First peak (L–L) and second peak (L–V) phase transition points [19]; (b) first peak (L–S) and second peak (L–V) phase transition points [18].

and Roux-Desgranges and Grolier [26]. Measured values of density and heat capacity were used to calculate the values of apparent molar volume and apparent molar heat capacity of species. The concentration dependences of these properties were analyzed in order to study of structural behavior of the microemulsions. The density and heat capacities per unit volume were measured over the whole miscibility region of the ternary system benzene–2-propanol–water by Lara et al. [27] at 25 °C. Unfortunately, all previous measurements were made at low temperatures (at 25 °C) and at low pressures (at atmospheric pressure). In the present work we studied the effect of high temperature (up to 525 K) and high pressure (up to 138 bar) on the thermodynamic and phase behavior of the microemulsion (water + *n*-octane + SDS + 1-pentanol). The results of the present work will be very useful for a better understanding the solubilization of hydrocarbons in micellar systems at high temperatures and high pressures.

2. Experimental

2.1. Construction of the calorimeter and principle of operation

The basic idea of the heat capacity measurements, details of the apparatus and procedures have been described in our several previous publications [6–17] and were used without modification; therefore, only essential information and brief description of them will be given here. Isochoric heat capacity–(C_VVTx) measurements near the phase transition points were performed on the high-temperature and high-pressure nearly constant-volume adiabatic calorimeter. The calorimeter is a multilayered system which consists of an internal thin-walled spherical vessel, outer adiabatic spherical shells, and a semiconductor layer (Cu_2O) between them. The internal spherical vessel is constructed of heat- and corrosion-resistant 1X18H9T stainless steel and has a volume of 105.405 cm^3. The sensor of the temperature difference (out-of-balance signal) between the calorimeter shell and the shield consisted of a five-junction copper-constantan thermopile whose signal is fed to an R-363/2 potentiometer, and from this potentiometer it is fed to a high precision temperature regulator (HPTR). The temperature difference between inner and outer shells was controlled within 5×10^{-3} K. If a layer of a semiconductor (Cu_2O) is placed between two concentric spherical vessels, the system will work as a highly sensitive thermoelement that can serve as a sensor detecting deviations from adiabatic conditions. The semiconductor layer simultaneously plays the role of a buffer that transmits pressure from the thin inner shell to the thicker outer shell. This makes it possible to increase the strength of the calorimeter without increasing its own heat capacity. Cuprous oxide (Cu_2O) has a very high thermoelectric power α (about 1150 V K^{-1}) in comparison with other semiconductors. This makes it possible to detect extremely small temperature differences (10^{-5} K) and eliminate heat transfer through the semiconductor layer. When making measurements near the phase transition points, the sample is vigorously mixed using a stirrer made of a thin perforated foil of stainless steel.

2.2. Constant-volume heat capacity measurements

Heat capacities at constant volume are obtained by measuring the heat (ΔQ, electrical energy released by the inner heater) input necessary to raise the temperature (ΔT, temperature change resulting from addition of an energy ΔQ) of a solution (m, mass of solution) contained in a spherical calorimeter and empty calorimeter heat capacity (C_0):

$$C_V = \frac{1}{m}\left(\frac{\Delta Q}{\Delta T} - C_0\right) \quad (1)$$

where the empty calorimeter heat capacity was calculated from the equation:

$$C_0 = 0.1244T - 1.037 \times 10^{-4}T^2 + 60.12 \quad (2)$$

where T is in K and C_0 is in $J\,K^{-1}$. The values of the empty calorimeter heat capacity were determined as a function of temperature by using (calibration procedure) the reference heat capacity data for He^4 [28] which is well known with an uncertainty of 0.2%. The uncertainty of temperature measurements was 15 mK. The detailed uncertainty analysis of the method (all of the measured quantities and corrections) is given in our several previous publications [13,15,16]. Based on a detailed analysis of all sources of uncertainties likely to affect the determination of C_V with the present system, the combined expanded ($k = 2$) uncertainty of measuring the heat capacity with allowance for the propagation of uncertainty related to the departure from true isochoric conditions of the heating process was 1.5–2.0% in liquid phase and 3–4% in the vapor phase.

Heat capacity is measured as a function of temperature at nearly constant density. The calorimeter was filled at room temperature, sealed off, and heated along a quasi-isochore. Each run for the heat capacity measurements was normally started in the two-phase (L–V, for completely miscibility systems) or in the three-phase (L–L–G, L–S–G, for partially miscibility systems) region and completed in the one-phase region (liquid or vapor depending on filling factor) at its highest temperature or pressure. Between initial (L–V, L–L–G, L–S–G) and final (one liquid or vapor phase) phase states the system undergoing various types phase transitions. This method enables one to determine, to a good accuracy, the transition temperature T_S and density at saturation ρ_S, the jump in the heat capacity ΔC_V, and reliable C_V data in the single-, two-, and three-phase regions for each quasi-isochore [6–17]. The one (vapor, C''_{V1} and liquid, C'_{V1})- and two (vapor + liquid, C''_{V2} and C'_{V2})-phase heat capacities at saturation, the saturated temperature (T_S), and saturated liquid (ρ'_S) and vapor (ρ''_S) densities can also be measured for solutions as discussed below (see below).

2.3. PVTx and $(\partial P/\partial T)_{VX}$ measurements

To measure of the volumetric properties we used above described calorimetric vessel as constant-volume piezometer. The density of the sample at a given temperature T and pressure P is calculated from the simple relation:

$$\rho = \frac{m}{V_{PT}} \tag{3}$$

where m is the filling mass of the sample in the calorimeter. The volume of the calorimeter at given T and P was calculated from

$$V_{PT} = V_{20} + \Delta V_{TP} \tag{4}$$

where $V_{20} = 105.405 \pm 0.01\ cm^3$ is the volume of calorimeter at a reference (room) temperature $t_0 = 20\,^\circ C$ and at atmospheric pressure (0.101325 MPa). The value of $V_{20} = m/\rho_{20}$, where $\rho_{20} = 998.2\ kg\,m^{-3}$ is the density of pure water at 20 °C and 0.101325 MPa and m is the mass of the water in calorimeter, previously calibrated from the known density of a standard fluid (pure water) with well-known (uncertainty is 0.0001% at 0.101325 MPa in the liquid phase) PVT values (IAPWS standard, Wagner and Pruß [29]). The pressure dependence of the calorimeter volume ΔV_P was calculated from the Love formula [30] for the sphere and by calibration procedure. The temperature expansion was obtained from the known expansion coefficient α_T of the calorimeter material (stainless steel 10X18H9T). The temperature and pressure dependence of the calorimeter volume was calculated as

$$\Delta V_{TP} = 0.0003(t - 20) + 0.0002(P - 0.1) \tag{5}$$

The volume at ambient conditions is known to 0.01%, the fill mass to 0.005%. The uncertainty of the pressure correction is estimated to be about 10%, and that of the temperature correction, 1.5%. Therefore, the uncertainty in the volume of the calorimeter at any T and P is 0.015%. The maximum uncertainty in density measurements is about 0.06%.

The pressure and temperature derivative of the pressure at constant volume and constant composition $(\partial P/\partial T)_{VX}$, were measured with individually calibrated extensometer. The pressure dependence of the departure electrical signal was described as linear function with uncertainty of 0.01%. The measurements of pressure in the calorimeter–piezometer were performed at constant temperature before each isochoric heat capacity measurements. Then, after turning on working heater the synchronously recording both temperature changes (thermograms, readings of the resistance thermometer PRT-10) and pressure changes (barograms, readings of the tenzotransducer) was performed with a strip-chart recorder. Using the records of the thermo-barograms the changes in temperature ΔT and in pressures ΔP, therefore the derivative $(\partial P/\partial T)_{VX} = \lim_{\Delta T \to 0} (\Delta P/\Delta T)_{VX}$, at any fixed time were calculated. The uncertainties of the direct temperature ΔT and pressure ΔP changes measurements are much accurate than the measurements of absolute values of the temperature and pressure. Therefore, the uncertainty in $(\partial P/\partial T)_{VX}$ is within 0.12–1.5% depending on the temperature increment (ΔT changes within 0.02–0.1 K). The uncertainty in pressure measurements is about 0.25%.

2.4. Phase boundary (T_S, P_S, ρ'_S,ρ''_S, C'_{VS}, and C''_{VS}) measurements: method of quasi-static thermograms

The method of quasi-static thermograms or isochoric heat capacity jumps in calorimetric C_VVTx experiment were used in this work to determine the location of the phase boundaries of the microemulsions (water + n-octane + SDS + 1-pentanol). The method of quasi-static thermograms (temperature *versus* time, T–τ plot) is used to accurate determines of the location of liquid–vapor (L–V) phase transition boundary for the complexity systems such as microemulsions (water + n-octane + SDS + 1-pentanol). The details and basic idea of the method of quasi-static thermograms and it application to complex thermodynamic systems are described in detail elsewhere [9,12,13,16–19].

The construction of the calorimeter described above enables to control the thermodynamic state of the measuring system with two independent sensors, namely, (1) a resistance thermometer-PRT-10 and (2) a layer of cuprous oxide surrounding the calorimetric vessel and serving as an adiabatic shield (inte-

grated adiabatic screen). Synchronously recording readings of the PRT-10 and of the sensor of adiabatic control, one can follow the thermodynamic state of the sample upon approaching the phase transition point. The method of thermograms (T–τ plot) is supplemented by recording readings of the sensor of adiabatic control; in combination, these ensure sufficient information on the changes in the sample thermodynamic state. On intersecting the phase transition curves (L–V–S, L–L–V, L–L–S, L–S, L–V), the heat capacity is known to change discontinuously, leading to a sharp change in the thermogram slope ($dT/d\tau$). The high sensitivity of cuprous oxide makes it possible to fix immediately the temperature changes on a strip-chart recorder. Temperature changes are recorded on a thermogram tape of a pen-recorder as a spike produced by the Cu_2O sensor and as a break (change of the thermogram slope). The Cu_2O responds to a change in the thermodynamic state of the sample at the internal surface of the calorimeter, while the resistance thermometer (PRT) records temperature changes in the center of the calorimeter. The presence of any temperature gradient in the volume of the sample would shift the positions of the spike and the break in the thermogram. However, with temperature changes occurring at rates of 5×10^{-5} to 10^{-4} K s^{-1}, the shift it observed to be less that 10^{-4} K.

The method of continuous heating in measuring heat capacity using adiabatic calorimeter allows one not only to accurately determine the phase transition temperature, but also directly measure, from the break in the thermogram, the magnitude of the heat capacity jump ΔC_V from the break of slopes of the thermograms as

$$\Delta C_V = k\left[\left(\frac{d\tau}{dT}\right)_{VT_S-0} - \left(\frac{d\tau}{dT}\right)_{VT_S+0}\right] \quad (6)$$

where $(d\tau/dT)_{VT_S-0}$ and $(d\tau/dT)_{VT_S+0}$ are the slopes of the thermograms before and after the phase transition point T_S, respectively, k a coefficient depending on the power of the heat flow and the mass of the sample studied, and T_S is the temperature of the phase transition corresponding to the fixed isochore V. The difference $[(d\tau/dT)_{VT_S-0} - (d\tau/dT)_{VT_S+0}]$ between thermogram slopes before $(d\tau/dT)_{VT_S-0}$ and after $(d\tau/dT)_{VT_S+0}$ phase transition is large enough (the changes in thermogram's slopes in liquid phase are within 20–30%). This is made easy and sensitive fixed any type phase transitions (detect even weak signs of a structural phase transition) occurring in the system.

Measurements of the temperatures and densities corresponding to the phase transition curve using the method of quasi-static thermograms in the above-described adiabatic calorimeter are carried out as follows. The calorimeter is filled with the solution to be studied until a necessary density is achieved; then, the apparatus is brought into the working range of temperatures and is held under adiabatic conditions for a sufficiently long time. After this, thermograms are recorded. At each isochore, thermograms are recorded several times during both heating and cooling. The retardation of the temperature run at T_{max} corresponds to a maximum in C_V, whereas a break at T_S corresponds to the intersection of the phase transition curve, where the heat capacity decreases discontinuously. In order to pass to another isochore, part of the sample is extracted from the calorimeter into a measuring vessel and the amount of the substance extracted is measured. This method of determination of the phase transition points has certain advantages over other methods; in particular, it has a high accuracy and reliability. The most widely used experimental method of determining parameters of the phase transition curve (coexistence curve) by the meniscus disappearance lacks objectivity. Moreover, with approaching the critical point, where the difference between the liquid and vapor phases vanishes, the visual determination of the moment at which the phase transition occurs becomes ever less reliable. In addition, the observations are impeded by the development of critical opalescence. Therefore, the region of temperatures near the critical point becomes virtually unattainable for investigation. The method under consideration makes it possible to obtain reliable data up to critical temperatures of $T_c \pm 0.01$ K.

To check and confirm the reliability and accuracy of the method and procedure of the phase boundary properties (T_S, ρ'_S, ρ''_S) measurements, measurements were made for pure water and toluene at selected densities with the same apparatus. The measurements were performed at two selected densities (214.64 and 555.25 kg m^{-3}) for toluene and (309.60 and 971.82 kg m^{-3}) for pure water. The measured values of phase transition temperatures for these densities are: T_S = 589.544 and 545.302 K for toluene and T_S = 647.090 and 353.060 K for pure water, respectively. These data were compared with the values calculated from reference equation of state for toluene by Lemmon and Span [31] and IAPWS formulation for pure water [29]. The difference between measured and calculated phase transition temperatures is good (0.2 K for toluene and 0.01 K for water). This good agreement for test measurements demonstrates the reliability and accuracy of the present method for phase transition and C_V measurements for water + n-octane + SDS + 1-pentanol solutions.

The compounds used were n-C_8H_{18} (99.8%), n-$C_5H_{11}OH$ (99.4%), and $C_{12}H_{25}OSO_3Na$ (99%). Triple-distilled water was used to prepare the solution samples.

3. Results and discussion

The thermodynamic properties ($PVTx$, P_S, T_S, ρ_S, $(\partial P/\partial T)_{VX}$, and $C_V VTx$) of three microemulsions (water + n-octane + SDS + 1-pentanol) with compositions: solution-1: 0.0777 (H_2O):0.6997 (n-C_8H_{18}):0.0777 (SDS):0.1449 (1-$C_5H_{11}OH$) mass fraction; solution-2: 0.6220 (H_2O):0.1555 (n-C_8H_{18}):0.0777 (SDS):0.1448 (1-$C_5H_{11}OH$) mass fraction; and solution-3: 0.2720 (H_2O):0.5054 (n-C_8H_{18}):0.0777 (SDS):0.1449 (1-$C_5H_{11}OH$) mass fractions were measured. Measurements were performed at six liquid densities (438.40, 475.87, 512.03, 710.58, 729.61, 743.38, 754.26, and 755.92 kg m^{-3}) for the solution-1 and one liquid isochores 919.03 and 815.66 kg m^{-3} for solution-2 and solution-3, respectively. The range of temperature was from 275 to 536 K. The experimental one-phase (liquid) and two-phase (liquid + vapor) $C_V VTx$, $PVTx$, $(\partial P/\partial T)_{VX}$ data and the values of (C_{V1}, C_{V2}, $(\partial P/\partial T)_{VX}$, P_S, T_S, ρ_S) at saturation are given in Supplementary Table 1 and Table 1 and shown in Figs. 3–5. Temperatures at

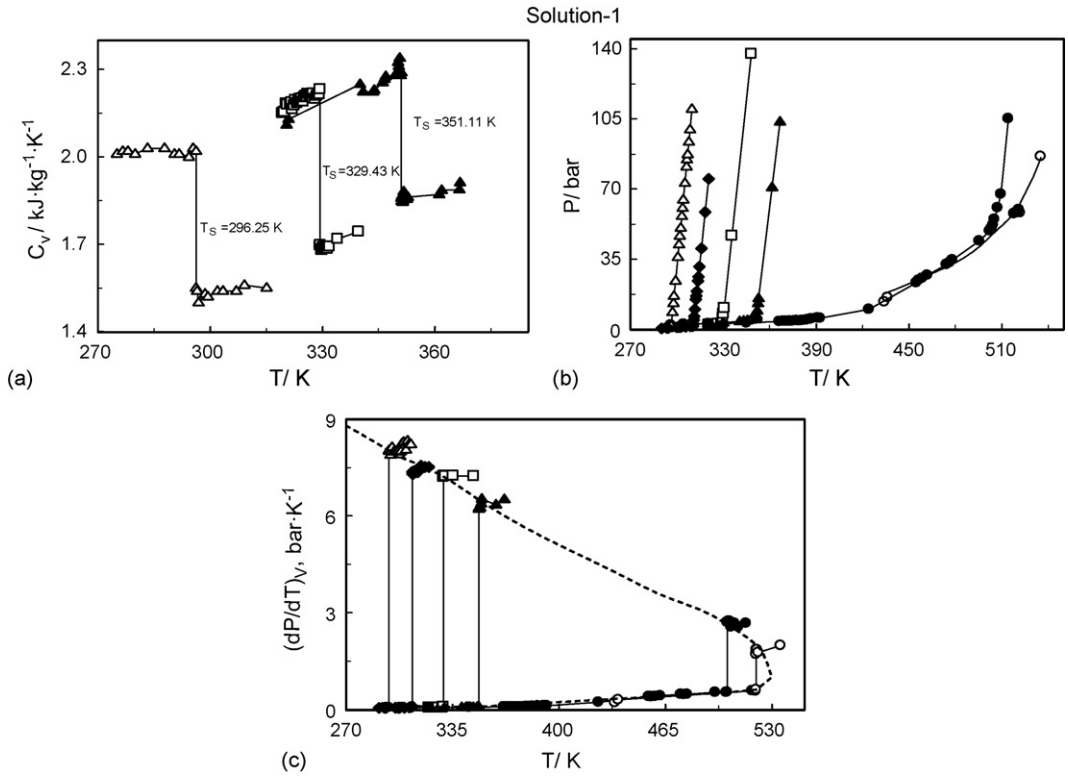

Fig. 3. Measured values of one- and two-phase isochoric heat capacities (a), pressures (b), and derivatives $(\partial P/\partial T)_{VX}$ (c) of quaternary solution-1 (water + *n*-octane + SDS + 1-pentanol) as a function of temperature T along the selected isochores near the phase transition points. (●) 512.03 kg m^{-3}; (◯) 475.87 kg m^{-3}; (△) 755.92 kg m^{-3}; (▲) 710.58 kg m^{-3}; (⧫) 744.40 kg m^{-3}; (□) 729.61 kg m^{-3}.

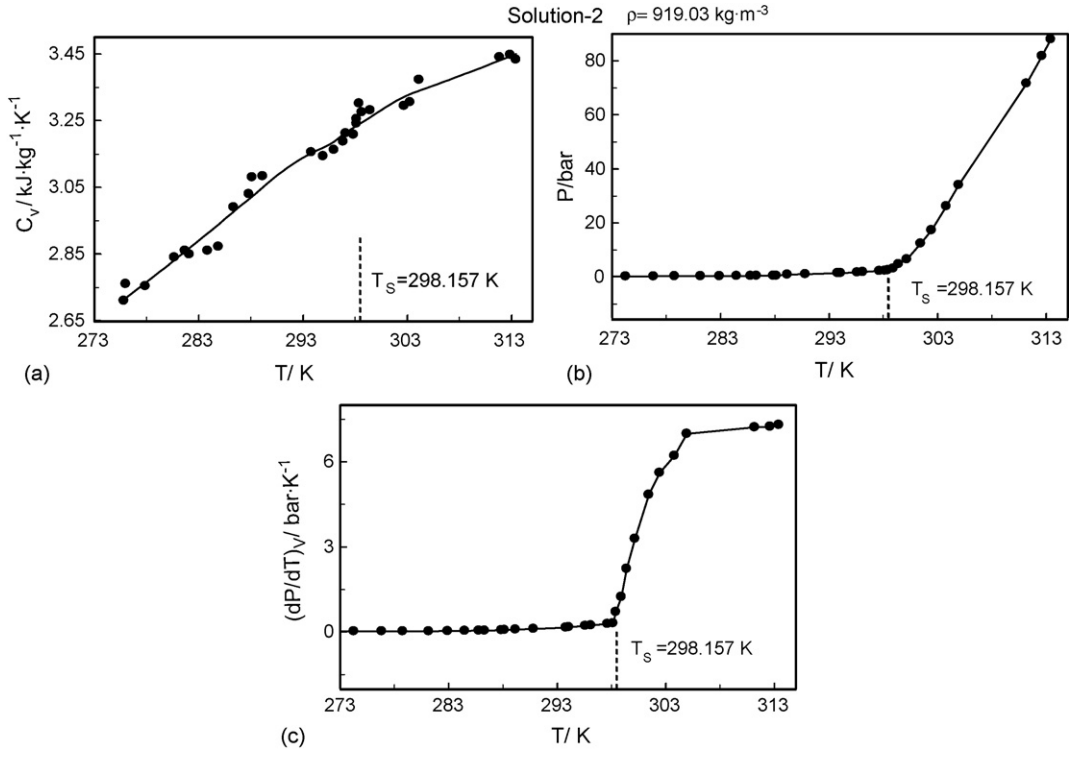

Fig. 4. Measured values of one- and two-phase isochoric heat capacities (a), pressures (b), and derivatives $(\partial P/\partial T)_{VX}$ (c) of quaternary solution-2 (water + *n*-octane + SDS + 1-pentanol) as a function of temperature T along the isochore of 919.03 kg m^{-3} near the phase transition point.

Table 1
Experimental thermodynamic properties (C'_{V1}, C'_{V2}, $(\partial P/\partial T)_{VX}$, T_S, P_S, ρ'_S, ρ''_S) of quaternary mixtures (water + n-octane + sodium dodecylsulfate + 1-pentanol) at saturation

T_S (K)	ρ'_S (kg m^{-3})	C'_{V1} (kJ kg^{-1} K^{-1})	C'_{V2} (kJ kg^{-1} K^{-1})	P_S (bar)	$(\partial P/\partial T)_{V2}$ (bar K^{-1})	$(\partial P/\partial T)_{V1}$ (bar K^{-1})
Solution-1						
296.248	755.92	1.55	2.02	0.650	0.060	8.02
310.569	744.40	1.63	2.14	1.720	0.100	7.37
329.426	729.61	1.70	2.23	2.530	0.090	7.22
351.109	710.58	1.86	2.29	5.090	0.090	6.22
503.716	512.03	2.87	3.39	50.66	0.541	2.71
520.478	475.87	2.93	2.93	58.43	0.620	1.82
Solution-2						
298.157	919.03	3.26	3.24	2.350	0.31	0.31
Solution-3						
289.955	815.66	2.88	3.11	0.430	0.09	8.12

the liquid + vapor phase transition curve (coexistence curve), $T_S(\rho)$, for each measured densities (isochores) are presented in Table 1 and in Fig. 6a together with values for the pure components calculated with equations of state [29,32] for n-octane and correlation [34] for 1-pentanol. The measured values of vapor-pressure for solution-1 and pure components calculated with [29,32,34] are presented in Fig. 6b. As shown in Figs. 3a and 5a for each isochore, the two-phase heat capacity C_{VX} drops discontinuously at the phase-transition temperature T_S to a value corresponding to that of the one-phase region (liquid phase). However, as one can see from Fig. 4a, for the solution-2 the jump in C_{VX} behavior has not been observed due to high concentration of water (0.622 mass fractions) and high density (919.03 kg m^{-3}). For each density at the phase-transition point T_S, we have two values of the heat capacity, namely C_{V1} and C_{V2}, corresponding to one- and two-phase states, respectively (see also Fig. 1). By changing the amount of sample in the calorimeter, it is possible to obtain a complete set of P_S, T_S, ρ_S, C_{V1} and C_{V2} data at saturation for each measured density (saturation curve or phase transition boundary curve). Thus, the C_{VX} experiments provide useful information about the saturation properties (phase transition boundary) (P_S, T_S, ρ_S, C_{V1} and C_{V2}) and phase diagram behavior. The measured values of the isochoric heat capacity C_{V1} and C_{V2} at phase transition curve as a function of temperature are plotted in Fig. 6c and d together with values for pure components (water and *n*-octane) calculated with equations of state [29,32]. *P–T* phase diagram for solution-1 is depicted in Fig. 3b. Figs. 4b and 5b

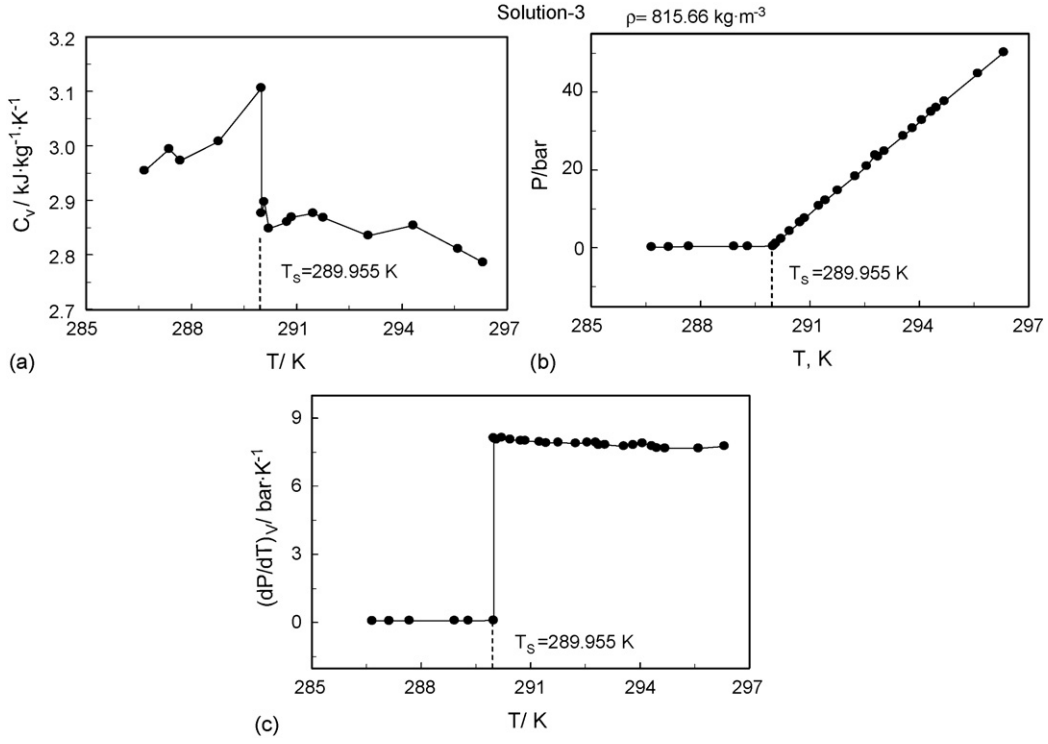

Fig. 5. Measured values of one- and two-phase isochoric heat capacities (a), pressures (b), and derivatives $(\partial P/\partial T)_{VX}$ (c) of quaternary solution-3 (water + *n*-octane + SDS + 1-pentanol) as a function of temperature *T* along the isochore of 815.66 kg m^{-3} near the phase transition point.

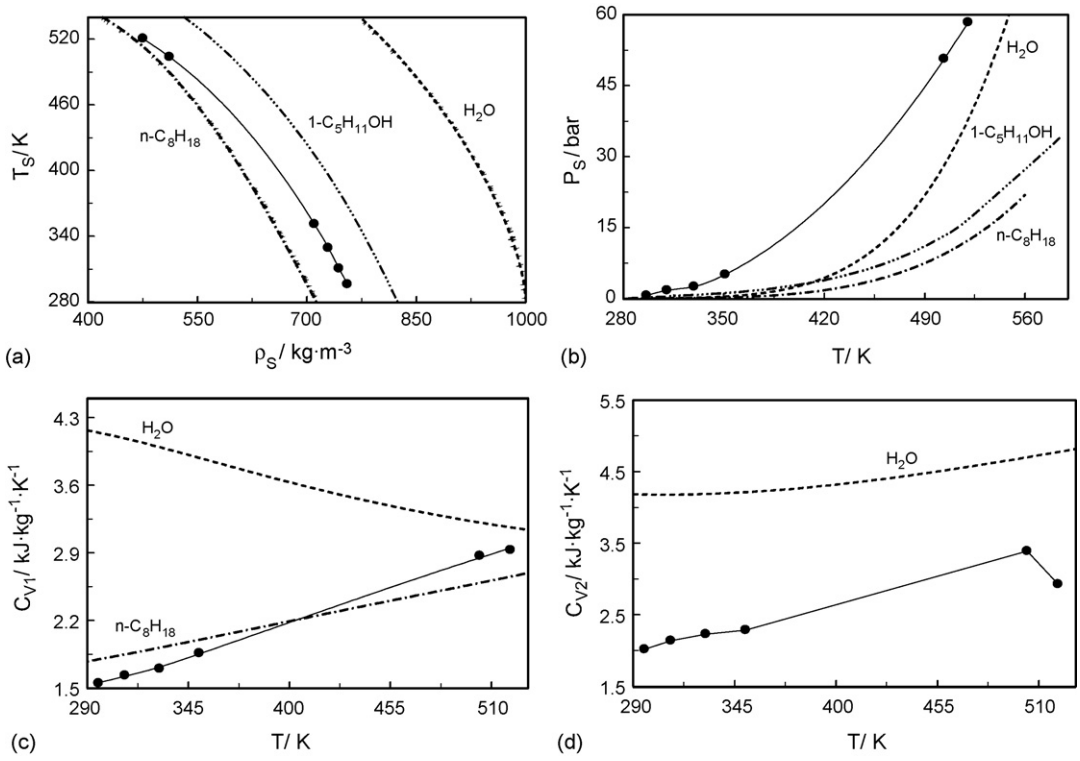

Fig. 6. Phase boundary properties, saturated density, T_S–ρ_S (a), vapor pressure, P_S–T_S (b), one-phase isochoric heat capacity, C_{V1}–T (c), and two-phase isochoric heat capacity, C_{V2}–T (d) of quaternary solution-1 (water + *n*-octane + SDS + 1-pentanol) together with pure components values (water [29], *n*-octane [31], and 1-pentanol [33,34]). (a) (●) experimental data for solution-1; (– – –) H_2O [29]; (– · – · –) *n*-C_8H_{18} [32]; (– · · · –) 1-$C_5H_{11}OH$ [34]. (b) (– – –) H_2O [29]; (– · – · –) *n*-C_8H_{18} [32]; (– · · · –) 1-$C_5H_{11}OH$ [33].

shows the *P*–*T* curves for two liquid isochores of 991.03 and 815.66 kg m^{-3} for solution-2 and solution-3, respectively. As one can see from these figures, at the phase transition temperatures T_S = 298.157 and 289.955 K the slope of *P*–*T* curve sharply changing (see also Figs. 4c and 5c). The break points in the *P*–*T* projection exactly the same as heat capacity jump points in calorimetric measurements (see Figs. 4a and 5a). As one can see from Fig. 4a, for high densities the isochoric heat capacity jump is small, while (see Fig. 4b) the slope changes at the break point (*P*–*T* projection) very markable. Therefore, at high densities (far from the critical point) *P*–*T* isochoric break point technique are more suitable to accurate determine of the phase boundary properties than quasi-static thermograms method. However, when approaching to the critical point the isochoric heat capacity jump, ΔC_V, therefore and the slope thermogram changes, $[(d\tau/dT)_{VT-\varepsilon} - (d\tau/dT)_{VT+\varepsilon}]$, diverge at the critical point as $\Delta C_V = k[(d\tau/dT)_{VT_S-\varepsilon} - (d\tau/dT)_{VT_S+\varepsilon}] \propto (T - T_C)^{-\alpha}$, where $\alpha = 0.112$ [35]. This is made easy and sensitive fixed any type phase transitions in the system near the critical point. *P*–*T* isochoric break points technique is less sensitive to phase transition in the critical region because the slope of the *P*–*T* curves changing very small due to the difference between densities of the phases (before and after phase transitions) is became very small. Therefore, method quasi-static thermograms methods more suitable to accurate determine of the phase boundary properties than *P*–*T* break point techniques in the critical region. The present constant-volume adiabatic calorimeter–piezometer technique allow to used simultaneously the both quasi-static thermogram and isochoric *P*–*T* break methods to accurate determine the location of the phase transition boundary for the complexity thermodynamic systems depending on the range of measurements.

Fig. 7 shows the temperature dependence of the isochoric heat capacity of solution-1 as a function of temperature along the isochore of 710.59 kg m^{-3} together with values for pure water

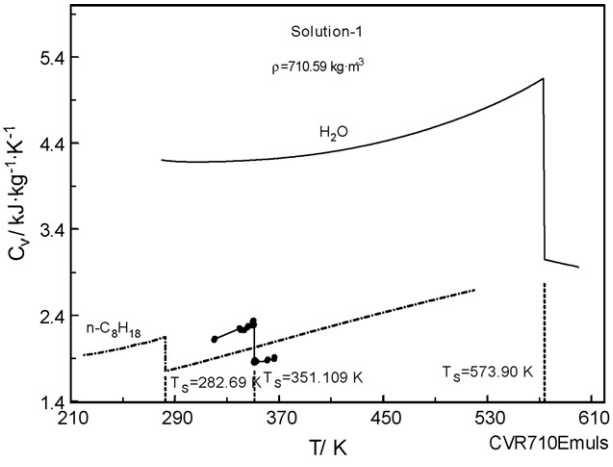

Fig. 7. Measured and calculated values of isochoric heat capacity of quaternary solution-1 (water + *n*-octane + SDS + 1-pentanol) and pure components as a function of temperature along the constant density of 710.59 kg m^{-3} near the phase transition temperatures. (●) experimental data for solution-1; (—) H_2O [29]; (– · – · –) *n*-C_8H_{18} [32].

and pure *n*-octane calculated with equation of state [29,32]. This figure demonstrate how changes the location of the phase transition temperatures of pure components (water and *n*-octane) and solution-1 at the same fixed density of 710.59 kg m^{-3}.

3.1. Phase transitions on isochoric heating

Several events occur when the fluid or fluid mixture is heated isochorically. Heating the pure fluids or fluid mixtures (completely miscible mixtures) in equilibrium with a vapor can lead to two different sequences of phase transitions, depending on the fill coefficient or the average fill density. The fill coefficient is defined as the ratio of the volume of the mixture to the volume of the vessel at ambient temperature. The average density equals the ratio of the mass of the mixture to the volume of the vessel at ambient temperature:

(1) At the highest measured densities ($\rho > \rho_C$, where ρ_C is the critical density), the liquid phase expands on heating and fills the entire vessel, while the vapor phase disappears. A transition (L–V ⇔ L) occurs, with a drop in heat capacity as the number of phases decreases (see Figs. 3a, 5a).
(2) At low measured densities ($\rho < \rho_C$), the vapor phase expands on heating and fills the entire vessel, while the liquid phase disappears. A transition takes place from two- to one-phase equilibrium (L–V ⇔ V), again with a drop of the heat capacity.

For more complicated multicomponent thermodynamic systems (for example, water + salt solutions with salt precipitation at high temperatures [18] or partially miscible liquids like water + hydrocarbon mixtures [19]) other sequences of phase transitions like L–V–S ⇔ L–V, L–V–S ⇔ L–S, L–V–S ⇔ V–S, L–L–S ⇔ L–L, L–L–S ⇔ L–S are possible (see Fig. 2). The sharp changes of measurable properties are connected with fluid–fluid and fluid–solid phase transitions occurring in a mixture heated in a closed volume (isochoric heating). An increase in the background level indicates an additional phase appearing, and a decrease indicates the disappearance of a phase.

For the all measured liquid isochores (solution-1), except 438.40 kg m^{-3}, the heating of the two-phase solution lead to jumps in the temperature dependence of isochoric heat capacity (see Fig. 3a, C_{VX}–T curves). The discontinuously changes of C_{VX} are connected with liquid–vapor phase transitions occurring in the solution heated in a closed volume. A transition takes place from two (L–V) to one (L) phase equilibrium (L–V ⇔ L), with a drop in heat capacity. However, on being heated at intermediate average densities (higher than critical), and before the thermal expansion causes the liquid to fill the entire volume, the initially unsaturated liquid solution becomes saturated with surfactant (SDS). In this case, the first phase transformation is the crystallization of solid from the liquid solution in equilibrium with its vapor (L–V ⇔ L–V–S), with an increase in heat capacity as the number of phases increases. On further heating of the solution, the concentration of the saturated liquid solution along the solubility curve decreases. Finally, the expanding liquid fills the cell save for the volume occupied by the solid surfactant. A transition from (L–V–S ⇔ L–S) equilibrium takes place, with a decrease in heat capacity. If the average fill density is somewhat lower than critical, the first transition is the appearance of solid salt (L–V ⇔ L–V–S), again with the heat capacity increasing. At higher temperatures, a second transition will correspond to disappearance of the liquid phase, a transformation of three-phase to two-phase (L–V–S ⇔ V–S) equilibrium, with a decrease in heat capacity.

The cases 1 have been encountered in the present experimental data for isochores (475.87, 512.03, 710.58, 729.61, 744.40 and 755.92 kg m^{-3}). However, for the isochore of 475.87 kg m^{-3} at temperatures around 520.478 K for the solution-1 the precipitation of the solid phase (SDS) was found. Unfortunately, we could not to continue the experiment for this isochore at temperatures above 520 K since surfactant (SDS) precipitation fouled calorimeter and plug connecting tubes.

4. Conclusions

In this work we provide comprehensive accurate experimental information on volumetric ($PVTx$), $(\partial P/\partial T)_{VX}$, calorimetric ($C_V VTx$), and phase boundary ($T_S$, P_S, ρ_S, x) properties data for complex quaternary solutions (water + *n*-octane + SDS + 1-pentanol) in the temperature range from 275 to 536 K and for densities between 475.87 and 919 kg m^{-3}. For each measured constant density (isochore) the liquid–vapor phase transition temperature, vapor pressure, one- and two-phase isochoric heat capacity values were determined. Along the isochore of 475.87 kg m^{-3} at temperatures around 520 K for solution-1 the precipitation of the solid phase (SDS) was found (liquid–vapor–solid or liquid–solid phase transition temperature).

Acknowledgements

One of us (IMA) thanks the Physical and Chemical Properties Division at the National Institute of Standards and Technology (NIST) for the opportunity to work as a contractor at NIST during the course of this research. This work was also supported by Grants RFBR 05-08-01149 and 05-08-18229-a.

Appendix A. Supplementary data

Supplementary data associated with this article can be found, in the online version, at doi:10.1016/j.tca.2006.12.014.

References

[1] L.M. Prince (Ed.), Microemulsions, Academic Press, New York, 1977.
[2] K.L. Mittal (Ed.), Micellization Solubilization and Microemulsion, Plenum Press, New York, 1976.
[3] K.L. Mittal (Ed.), Solution Chemistry of Surfactants, Plenum Press, New York, 1979.
[4] J.E. Desnoyers, R. Beaudoin, G. Perron, G. Roux, Chemistry for Energy, in: M. Tomlinson (Ed.), ACS Sym. Series 90, ACS, Washington, DC, 1979, p. 35.
[5] R.L. Berg, L.A. Noll, W.O. Good, Chemistry of oil recovery, in: R.T. Johansen, R.L. Berg (Eds.), ACS Sym. Series 91, ACS, Washington, DC, 1979, p. 81.

[6] N.G. Polikhronidi, I.M. Abdulagatov, J.W. Magee, G.V. Stepanov, Int. J. Thermophys. 22 (2001) 189.
[7] N.G. Polikhronidi, I.M. Abdulagatov, J.W. Magee, G.V. Stepanov, Int. J. Thermophys. 23 (2002) 745.
[8] N.G. Polikhronidi, I.M. Abdulagatov, J.W. Magee, G.V. Stepanov, Int. J. Thermophys. 24 (2003) 405.
[9] N.G. Polikhronidi, I.M. Abdulagatov, R.G. Batyrova, Fluid Phase Equilib. 201 (2002) 269.
[10] N.G. Polikhronidi, R.G. Batyrova, I.M. Abdulagatov, Int. J. Thermophys. 21 (2000) 1073.
[11] N.G. Polikhronidi, R.G. Batyrova, I.M. Abdulagatov, J.W. Magee, G.V. Stepanov, J. Supercrit. Fluids 33 (2004) 209.
[12] N.G. Polikhronidi, R.G. Batyrova, I.M. Abdulagatov, Fluid Phase Equilib. 175 (2000) 153.
[13] B.A. Mursalov, I.M. Abdulagatov, V.I. Dvoryanchikov, S.B. Kiselev, Int. J. Thermophys. 20 (1999) 1497.
[14] I.M. Abdulagatov, S.B. Kiselev, J.F. Ely, N.G. Polikhronidi, A.A. Abdurashidova, Int. J. Thermophys. 26 (2005) 1327.
[15] I.M. Abdulagatov, B.A. Mursalov, V.I. Dvoryanchikov, J. Chem. Eng. Data 45 (2000) 1133.
[16] Kh.I. Amirkhanov, G.V. Stepanov, I.M. Abdulagatov, O.A. Buoi, in: V.V. Sychev (Ed.), Isochoric Heat Capacity of Propan-1-ol and Propan-2-ol, Russian Academy of Sciences, Makhachkala, 1989.
[17] Kh.I. Amirkhanov, G.V. Stepanov, B.G. Alibekov, Isochoric Heat Capacity of Water and Steam, Amerind Publ. Co., New Delhi, 1974.
[18] V.M. Valyashko, I.M. Abdulagatov, J.M.H. Levelt-Sengers, J. Chem. Eng. Data 45 (2000) 1139.
[19] I.K. Kamilov, G.V. Stepanov, I.M. Abdulagatov, A.R. Rasulov, E.I. Milikhina, J. Chem. Eng. Data 46 (2001) 556.
[20] M.A. Urusova, V.M. Valyashko, Russ. J. Inorg. Chem. 46 (2001) 777.
[21] A.R. Bazaev, I.M. Abdulagatov, J.W. Magee, E.A. Bazaev, A.E. Ramazanova, Int. J. Thermophys. 25 (2004) 804.
[22] N.G. Stretenskaya, R.J. Sadus, E.U. Franck, J. Phys. Chem. 99 (1995) 4273.
[23] A.H. Roux, G. Roux-Desgranges, J-P.E. Grolier, A. Viallard, J. Colloid Interf. Sci. 84 (1981) 250.
[24] G. Roux-Desgranges, A.H. Roux, J-P.E. Grolier, A. Viallard, J. Colloid Interf. Sci. 84 (1981) 536.
[25] G. Roux-Desgranges, A.H. Roux, J-P.E. Grolier, A. Viallard, J. Solid Chem. 11 (1982) 357.
[26] G. Roux-Desgranges, J. Grolier, Fluid Phase Equilib. 25 (1986) 209.
[27] J. Lara, G. Perron, J.E. Desnoyers, J. Phys. Chem. 85 (1981) 1600.
[28] N.B. Vargaftik, Handbook of Physical Properties of Liquids and Gases, 2nd ed., Hemisphere, New York, 1983.
[29] W. Wagner, A. Pruß, J. Phys. Chem. Ref. Data 31 (2002) 387.
[30] F.G. Keyes, L.B. Smith, Proc. Am. Acad. Arts Sci. 68 (1933) 505.
[31] E.W. Lemmon, R. Span, J. Chem. Eng. Data 51 (2006) 785.
[32] R. Span, W. Wagner, Int. J. Thermophys. 24 (2003) 41.
[33] D. Ambrose, J. Walton, Pure Appl. Chem. 61 (1989) 1395.
[34] I. Cibulka, Fluid Phase Equilib. 89 (1993) 1.
[35] J. Rowlinson, F.L. Swinton, Liquids and Liquid Mixture, 3rd ed., Butterworths, London, 1982.